

S. STRZELECKI*, S.M. GHONEAM**

The effect of clearance variation on the maximum temperature of the oil film of cylindrical 3-lobe journal bearing

Key words

Theory of lubrication, multilobe journal bearings, maximum oil film temperature.

Słowa kluczowe

Teoria smarowania, łożyska ślizgowe wielopowierzchniowe maksymalna temperatura filmu smarowego.

Summary

The variation of the journal bearing clearance has an effect on the bearing operation. It should be strictly controlled to avoid unexpected failures of the bearing. The changes in the clearance of the bearing cause the changes in its static and dynamic characteristics. An effect of the clearance on the oil-film temperature distribution and its maximum value is very important. The full characteristics of 3-lobe cylindrical journal bearings are not accessible in practice.

The paper presents the results of the theoretical investigation into an effect of bearing clearance on the oil film temperature distribution and its maximum value of 3-lobe cylindrical journal bearing. The oil film pressure and temperature distributions were obtained by numerical solution of the Reynolds, energy, and viscosity equations with the geometry equation.

* Department of Machine Design, Lodz University of Technology, Lodz, Poland.

** Mechanical Design & Production Engineering Department, Faculty of Engineering, El-Monoufia University, Shebin-El-Kom, Egypt.

1. Introduction

The 3-lobe journal bearings [1-3] that are applied in the turbines and turbo-generators should assure long and reliable operation of this rotating machinery. As compare to the bearings with cylindrical bushes, they are characterised by good stability in the range of higher rotational speeds, assuring very good cooling conditions for the oil film. Any failure occurring during operation of these bearings can cause very high power loses. The part of static characteristics of the journal bearings consists of the oil film maximum temperature, which is very important factor in the process of reliable bearing design and others.

The 3-lobe bearings include the 3-lobe cylindrical bearing [1], classic bearing [1-2] or pericycloid bearing [3-5]. All these types of bearings have three lubricating pockets placed at 120°. The characteristic feature of classic 3-lobe bearing is the difference in radii between them. The single lobes of this bearing are designed as the arc of the circle with the centre points placed on the symmetry line of the single lobe. In the symmetric multilobe bearing, the circle inscribed in the bearing profile is tangent to the lobe exactly at the middle point of each lobe. In case of 3-lobe cylindrical bearing, the inscribing radius and the lobe radius are equal, and this bearing is designed as three parts bearing of cylindrical non-continuous profile [1].

The paper introduces theoretical investigation into the maximum oil film temperature of 3-lobe, cylindrical journal bearings. The Reynolds, energy, and viscosity equations were solved numerically on the assumption of incompressible lubricant, and on the laminar and adiabatic flow of oil in the lubricating gap of finite length bearing. The static equilibrium position of the journal was assumed in the calculations [1-5].

2. Oil film pressure and temperature distribution

On the assumption of the parallel axis of journal and bearing sleeve, the geometry of oil film gap of multilobe journal bearing (Fig. 1) is described by Equation (1) [1, 2].

$$\bar{H}(\varphi) = \bar{H}_{Li}(\varphi) - \varepsilon \cdot \cos(\varphi - \alpha) \quad (1)$$

Where: α – attitude angle, (°), ε – relative eccentricity, φ – peripheral coordinate, (°)

The first member of the right side of Equation (1) that determines the geometry of 3-lobe classic journal bearing, at the concentric position of journal and bearing axis, has the following form [1, 2]:

$$\bar{H}_{Li}(\varphi) = \psi_{si} + (\psi_{si} - 1) \cdot \cos(\varphi - \gamma_i) \quad (2)$$

Where: γ_i – angle of lobe centre point, ($^{\circ}$), ψ_{si} – lobe relative clearance ($\psi_{si} = 1$ for cylindrical bearing)

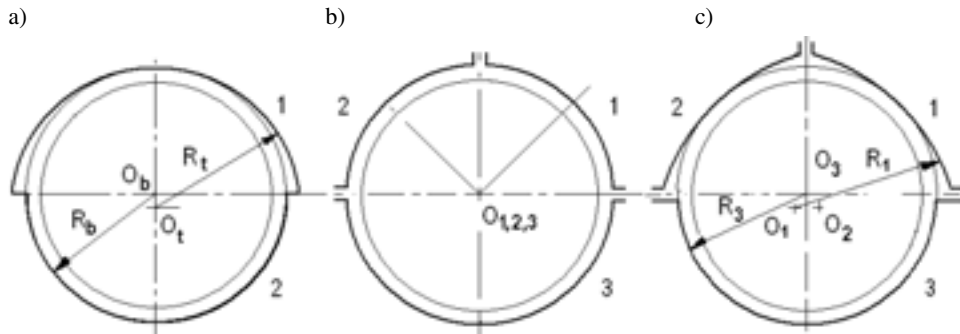


Fig. 1. Examples of multilobe journal bearings: a) half-lemon, b) cylindrical 3-pockets, c) 3-lobe asymmetrical (combined profile); R_t , R_b – radius of upper and bottom lobe, O_b , O_t – centre of bearing (centre of bottom lobe) and upper lobe, O_1 , O_2 , O_3 – centres of lobes

Fig. 1. Przykłady łożysk ślizgowych wielopowierzchniowych: a) cytrynowo-cylindryczne, b) cylindryczne 3-kieszeniowe, c) 3-powierzchniowe asymetryczne (profil kombinowany); R_t , R_b – promień segmentu górnego i dolnego, O_b , O_t – środek łożyska (segmentu dolnego) i, segmentu górnego, O_1 , O_2 , O_3 – środki segmentów

The journal bearing performances for the adiabatic model of oil film can be determined by the numerical solution of the oil film geometry, Reynolds, energy, and viscosity equations. The oil film pressure distribution was defined from transformed Reynolds Equation (3) [1-6].

$$\frac{\partial}{\partial \varphi} \left(\frac{\bar{H}^3}{\bar{\eta}} \frac{\partial \bar{p}}{\partial \varphi} \right) + \left(\frac{D}{L} \right)^2 \frac{\partial}{\partial \bar{z}} \left(\frac{\bar{H}^3}{\bar{\eta}} \frac{\partial \bar{p}}{\partial \bar{z}} \right) = 6 \frac{\partial \bar{H}}{\partial \varphi} + 12 \frac{\partial \bar{H}}{\partial \phi} \quad (3)$$

Where: D , L – bearing diameter and length (m), $\bar{H} = h/(R-r)$ – dimensionless oil film thickness, h – oil film thickness (μm), \bar{p} – dimensionless oil film pressure, $\bar{p} = p\psi^2/(\eta\omega)$, p – oil film pressure (MPa), r , R – journal and sleeve radius (m), φ , \bar{z} – peripheral and dimensionless axial co-ordinates, ϕ – dimensionless time, $\phi = \omega t$, t – time (sec), ω – angular velocity (sec^{-1}), $\bar{\eta}$ – dimensionless viscosity, ψ – bearing relative clearance, $\psi = \Delta R/R$ (%), ΔR – bearing clearance, $\Delta R = R - r$ (m).

It has been assumed for the pressure region that, on the bearing edges and in the regions of negative pressures, the oil film pressure $\bar{p}(\varphi, \bar{z}) = 0$. The oil film pressure distribution computed from Equation (3) was put in the transformed energy Equation (4) [6,7].

$$\begin{aligned} \frac{\bar{H}}{Pe} \left[\frac{\partial^2 \bar{T}}{\partial \varphi^2} + \left(\frac{D}{L} \right)^2 \frac{\partial^2 \bar{T}}{\partial \bar{z}^2} \right] + \left[\frac{\bar{H}^3}{12\bar{\eta}} \frac{\partial \bar{p}}{\partial \varphi} - \frac{\bar{H}}{2} \right] \frac{\partial \bar{T}}{\partial \varphi} + \left(\frac{D}{L} \right)^2 \frac{\bar{H}^3}{12\bar{\eta}} \frac{\partial \bar{p}}{\partial \bar{z}} \frac{\partial \bar{T}}{\partial \bar{z}} = \\ = - \frac{\bar{H}^3}{12\bar{\eta}} \left[\left(\frac{\partial \bar{p}}{\partial \varphi} \right)^2 + \left(\frac{D}{L} \right)^2 \left(\frac{\partial \bar{p}}{\partial \bar{z}} \right)^2 \right] - \frac{\bar{\eta}}{\bar{H}} \end{aligned} \quad (4)$$

Where: \bar{T} – dimensionless oil film temperature, Pe – Peclet number,

Oil film temperature and viscosity fields were obtained by numerical solving of Equation (3) and Equation (4). The temperature $T(\varphi, \bar{z})$ on the bearing edges ($\bar{z} = \pm 1$) was computed by the method of parabolic approximation [6, 7]. The developed program of numerical calculation [2, 6] solves all of the above-mentioned equations.

3. Results of calculations

The calculations included the non-dimensional load capacity S_0 and journal displacement ε , the static equilibrium position angles α_{eq} , and oil film pressure and temperature distributions. The assumed values of bearing length to diameter ratios were $L/D = 0.5$ and $L/D = 0.8$, and, at the bearing relative clearances, $\psi = 1.5\%$ and $\psi = 2.7\%$, and the lobe relative clearances $\psi_s = 1$. The rotational speed of the journal was $n = 3000$ rpm. The temperature of feeding oil was $T_0 = 40^\circ\text{C}$.

Calculations of oil film maximum temperatures were carried out for the range of relative eccentricities $\varepsilon = 0.1$ to $\varepsilon = 0.8$. Vertical direction of load $\beta = 270^\circ$, directed on the bottom lobe (Fig. 1b and Fig. 1c – lobe No. 3) was assumed.

Exemplary results of the calculations of static characteristics and oil film maximum temperature are shown in Fig. 2 through Fig. 7. The comparison of journal displacements ε and static equilibrium position angles α_{eq} versus Sommerfeld number S_0 , for different 3-lobe bearings, are showed in Fig. 2 and Fig. 3, respectively (in Fig. 2 through Fig. 5 - 3LC – 3-lobe cylindrical, 3LM - 3-lobe). The smallest displacements (Fig. 2) and static equilibrium position angles (Fig. 3) are observed in case of 3-lobe cylindrical bearing.

The effect of bearing relative clearance ψ on the journal displacements and maximum oil film temperature are presented in Fig. 4 and Fig. 5. An increase in the bearing relative clearance ψ causes the decrease in the calculated parameters in all ranges of Sommerfeld numbers.

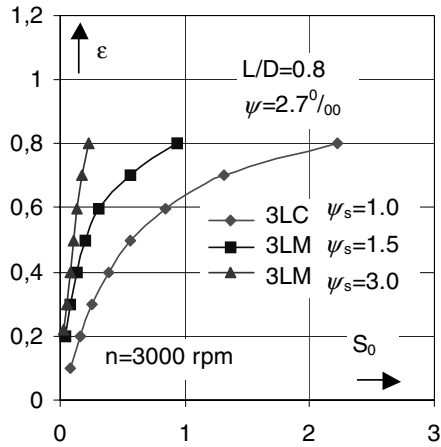


Fig. 2. Journal eccentricity versus Sommerfeld number

Rys. 2. Przemieszczenie czopa w funkcji położenia równowagi liczby Sommerfelda

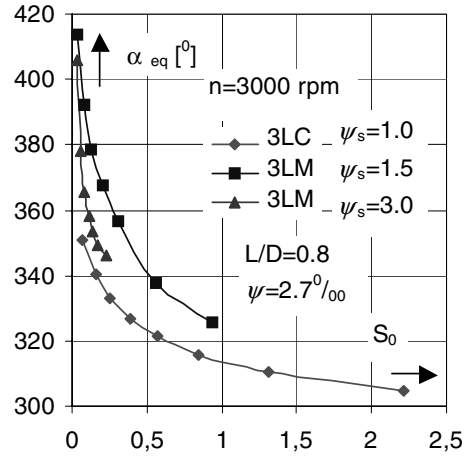


Fig. 3. Static equilibrium position angles versus Sommerfeld number

Rys. 3. Statyczny kąt w funkcji liczby Sommerfelda

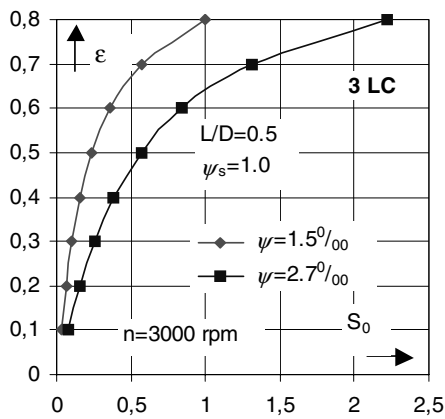


Fig. 4. Journal eccentricity versus Sommerfeld number

Rys. 4. Przemieszczenie czopa w funkcji liczby Sommerfelda

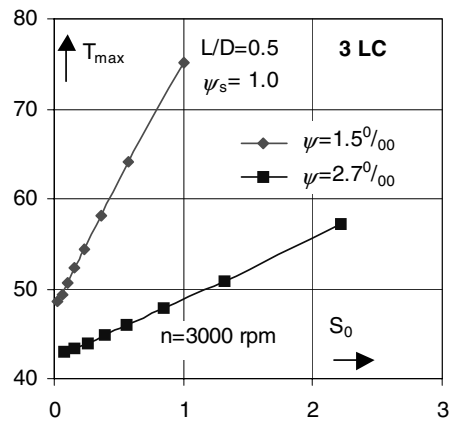


Fig. 5. Maximum oil film temperature versus Sommerfeld number

Rys. 5. Maksymalna temperatura filmu smarowego w funkcji liczby Sommerfelda

The calculated oil film pressure and temperature distributions in 3-lobe cylindrical journal bearing are presented in Fig. 6 and Fig. 7 at different values of the bearing relative clearance.

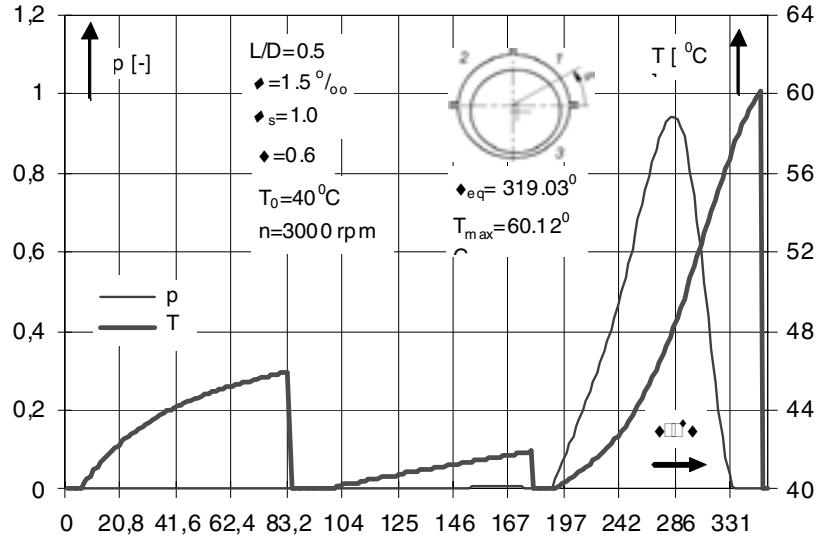


Fig. 6. Oil film pressure and temperature distributions in 3-lobe cylindrical journal bearing $\psi=1.5\text{‰}$
 Rys. 6. Rozkład ciśnienia i temperatury w filmie smarowym łożyska 3-powierzchniowego z cylindrycznym zarysem panewki dla względnego luzu łożyskowego $\psi=1,5\text{‰}$

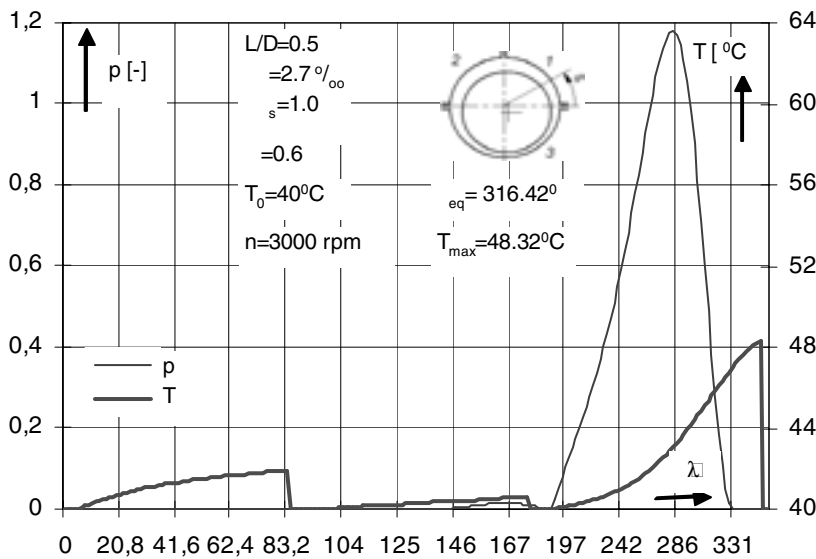


Fig. 7. Oil film pressure and temperature distributions in 3-lobe cylindrical journal bearing $\psi=2.7\text{‰}$
 Rys. 7. Rozkład ciśnienia i temperatury w filmie smarowym łożyska 3-powierzchniowego z cylindrycznym zarysem panewki dla względnego luzu łożyskowego $\psi=2,7\text{‰}$

4. Final remarks

It results from the carried out calculations that the bearing relative clearance has an effect on the bearing performances. An increase in the bearing relative clearance ψ causes the decrease in the journal displacements, static equilibrium position angles, oil film pressure and temperature distributions and their maximum values in all range of considered Sommerfeld numbers.

The correct operation of the developed code of calculations was checked in experimental investigations [4, 5] on the oil film temperatures of pericycloid 3-lobe journal bearings that were applied in the real mechanical system of grinding spindle. In such a bearing system, the temperatures of the oil film are affected by many factors, e.g., casing design, the temperature of supplied oil, and its pressure. However, the results that were obtained in experimental investigations [4, 5] were comparable to the computed ones with the correct values of maximum temperatures on the bearing lobes.

References

- [1] Han D.C., Statische und dynamische Eigenschaften von Gleitlagern bei hohen Umfangsgeschwindigkeiten und bei Verkanntung Diss. TU Karlsruhe. Karlsruhe. (1979).
- [2] Strzelecki S., Design of the tribosystem of 3-lobe journal bearing. Tribologia R.28 nr 4. (1997). 323-332.
- [3] Dimofte F., Wave Journal Bearing with Compressible Lubricant- Part I: The Wave Bearing Concept and a Comparison to the Plain Circular Bearing. Tribology Transaction Vol.38. (1995). 153-160.
- [4] Strzelecki S., Socha Z., Effect of Load Direction on the Oil Film Temperature Distribution of 3-Lobe Pericycloid Journal Bearing. Technical University Ostrava. PIME2009. Trans. of Tech. Univ. Ostrava. Metallurg. Ser. 2009. R.52 No. 3. (2009). 211-216.
- [5] Strzelecki S., Socha Z., Effect of feeding oil pressure on the oil film temperature of 3-lobe pericycloid bearing. INTERTRIBO 2009. October 21-23.2009. Slovak Republik. Proceedings of the Conference. (2009). 33 - 36.
- [6] Ghoneam S. M., Strzelecki S., Thermal Problems of Multilobe Journal Bearings. Meccanica. DOI 10.1007/s11012-006-9004-z. 41. Springer. (2006). 571-579.
- [7] Strzelecki S., Towarek Z., Oil film temperature of high-speed cylindrical journal bearing. Proc. of the International Conference SLAVYANTRIBO'7. Sankt Petersburg. Russia. Vol. 2. (2006). 22-29.

Manuscript received by Editorial Board, March 22rd, 2010

Wpływ zmian luzu łożyskowego na maksymalną temperaturę filmu smarowego 3-powierzchniowego cylindrycznego łożyska ślizgowego

Streszczenie

Ślizgowe łożyska 3-powierzchniowe stosowane są w odpowiedzialnych układach łożyskowych turbin parowych, turbogeneratorów i sprężarek. Łożyska te w porównaniu z łożyskami o panewce cylindrycznej charakteryzują się lepszą statecznością w zakresie wyższych

prędkości obrotowych, obciążeń oraz zapewniają bardzo dobre warunki chłodzenia filmu smarowego. Łożyska 3-powierzchniowe reprezentowane są przez łożyska z panewką cylindryczną i trzema kieszeniami smarowymi, łożyska z panewką pericykloidalną oraz łożyska typu „offset” (z przesuniętymi w płaszczyźnie poziomej segmentami). Łożyska 3-powierzchniowe z zarysem cylindrycznym są łożyskami o nieciągłym zarysie panewki w kierunku obwodowym oraz są technologicznie łatwe w wykonaniu.

Znajomość rozkładu temperatury w filmie smarowym cylindrycznego łożyska 3-powierzchniowego oraz wartości maksymalnej temperatury dla różnych parametrów geometrycznych oraz eksploatacyjnych umożliwia wybór konstrukcji łożyska spełniającej warunki długiej i niezawodnej pracy. Zmiana luzu łożyskowego wpływa na charakterystyki statyczne i dynamiczne łożyska, na rozkład temperatury w filmie smarowym i jej wartość maksymalną.

Z przeprowadzonych obliczeń oraz analizy wynika, że zmiana luzu łożyskowego wpływa na wartość maksymalną temperatury filmu smarowego. Jest to szczególnie istotne w przypadku rozpatrywanego łożyska 3-powierzchniowego o zarysie cylindrycznym – łożyska takie ze względu na prostą konstrukcję i niski koszt wykonania mogą być stosowane w odpowiedzialnych, wysokoobrotowych maszynach wirnikowych.